Proceedings of the ASME 2023
50th Annual Review of Progress in
Quantitative Nondestructive Evaluation
QNDE2023
July 24-27, 2023, Austin, Texas

QNDE2023-108496

MEASUREMENT SYSTEM ANALYSIS OF A NOVEL PHASE-BASED ULTRASONIC NDE TECHNIQUE FOR BOND STRENGTH MEASUREMENT

Peter Takunju[1], Matthew Webster[1], Joseph Zalameda[1]

[1]NASA Langley Research Center, Hampton, VA, USA

ABSTRACT

Fiber reinforced polymer parts have shown tremendous benefits in aerospace structural applications, but their qualification and certification for use in safety critical areas are currently hindered by the lack of a capable non-destructive evaluation (NDE) method or technique for the inspection of these adhesively bonded parts. Conventional NDE methods and techniques typically detect gross bond defects in a qualitative (Pass/Fail) manner. These techniques struggle to detect weak or kissing bonds. Also, there are no widely adopted NDE methods or techniques for measuring interfacial bond strength or detecting kissing bonds. Bond strength is currently ensured by process control and semi-destructive testing. Results from recent research from other authors, including but not limited to mechanical testing, have shown an excellent correlation between interfacial stiffness of an adhesively bonded joint and the adhesive bond strength of that joint. In this paper, a measurement system analysis (MSA) of a novel phase-based ultrasonic NDE Technique, developed at NASA Langley Research Center, is presented for bond strength measurements to assess at an increased level the measurement process and identify components of variation in the process.

Keywords: Ultrasound, Adhesive Bond, Interfacial Stiffness, Bond Strength, Phase Locked Loop

1. INTRODUCTION

The use of bonded composite joints in next generation aircraft is expected to increase as these lightweight adhesively-bonded parts have shown some great benefits including improvements in mechanical properties, fuel efficiency, flight range and payload which consequently reduces aircraft operation costs [1]. Also, due to the ability to distribute load over a much broader area, adhesively bonded joints are considered more efficient than mechanical joints [2]. However, the development, qualification and mainstream adoption of these adhesively bonded composite joints is being impeded by the lack of a reliable and quantitative nondestructive evaluation (NDE) method or technique for quality assurance of these parts. A comprehensive review of the defects and uncertainties associated with adhesively bonded composite joints is given in [3]. Currently, commercial NDE methods and techniques can readily detect bonding issues in adhesively bonded joints, for example gross defects and delaminations, albeit in a more qualitative (Pass/Fail) manner. However, they are not capable of detecting weak or kissing bonds in adhesively bonded joints. Manufacturing defects can create weak bonds that could be catastrophic, and such severity coupled with detection challenges makes these types of bonds one of the most critical defects in adhesively bonded joints [4-5]. In fact, though bond quality control in manufacturing and production of these bonded composite joints is currently still being determined by process control and destructive testing through sampling, there have been numerous studies over several decades devoted to the NDE of kissing bonds and other bond types [6-10]. With most previous research work being more qualitative in nature, there remains that critical need for a quantitative nondestructive assessment of an adhesively bonded joint which is essential to the qualification and certification of these composite parts for use. A comprehensive overview of major nondestructive testing and proof testing methods for sizing disbonds and determining bond strength of weak bonds is given in [11] with their limitations. A more promising technique for detecting weak bond has been developed based on a physics-based modeling framework that describes an adhesive bond as a distribution of massless springs, relating acoustic response to mechanical connection between adhesive and adherent [6, 13]. Following this framework, the interfacial stiffness of the spring network model was found to be related to the number of chemical bonds per unit area and having a direct relation to bond strength [14].

A novel phase-based ultrasonic technique, based on a constant

 © 2023 by ASME

frequency phase-locked loop (CFPLL) technology, was recently developed at NASA Langley Research Center (LaRC) [15]. This novel technique has shown the ability to measure interfacial bond strength using swept-frequency ultrasonic phase measurements of bondline reflections and observing how changes in interfacial stiffness affect phase response near ultrasonic resonance of the bondline [16]. The technique was experimentally demonstrated in a prior study using Borofloat[ϕ] glass adherents bonded with UV-curable Norland optical adhesive (NOA60) in a simple bonded joint to characterize its bonding quality via an interfacial stiffness metric. Experimental results from this study have shown a strong positive linear relationship between the ultrasonically-measured interfacial stiffness and mechanically-measured bond strength [17]. Though still an emerging measurement technique, the MSA study in this paper evaluates the phase-based NDE method for quantitative bond quality assessment to ensure the integrity of data used for quality analysis and to develop an understanding of how measurement errors could affect data-driven decisions. In the study presented in this paper, the interfacial stiffnesses of both FM209-1U and NOA60 adhesives were assessed using the novel Phase-Based Ultrasonic system. Eight coupons were made from borosilicate glass adherents bonded by the FM209-1U and NOA60 adhesives. Four more coupons were made with epoxy adhesive. These twelve samples in total were made with varying bond quality including varying amount of curing and degradation through inadequate surface preparation and contamination. Repeated, randomized measurements (3 replicates per sample) were obtained from these samples by two different operators and collected data were analyzed by the ANOVA (Analysis of Variance) method using Minitab®[ϕ] with the goal to quantify measurement precision namely, repeatability and reproducibility, of this novel device.

2. TECHNICAL BACKGROUND

2.1 Physics-Based Model of Adhesion

Figure 1 is an illustration of a tri-layer adhesively bonded joint where adhesion is modeled by a massless spring network of mechanical connections between the adhesive and adherents [18]. The interfacial adhesive bond quality is represented by the interfacial stiffness (K_1=K_2=K), defined as the stiffness per unit area. According to Tattersal's simplified model, for a given normally incident ultrasonic wave, the complex reflection coefficient R of the modeled tri-layer imperfect interfaces is given by [6]:

$$R = \frac{Z_1 - Z_2 + i\omega\frac{Z_1 Z_2}{K}}{Z_1 + Z_2 + i\omega\frac{Z_1 Z_2}{K}} \quad (1)$$

where Z_1 and Z_2 are the acoustic impedances of the respective interfacing layer; and ω is the wave's angular frequency. According to Equation (1), we get a complete disbond as K→0 and a perfect interface as K→∞.

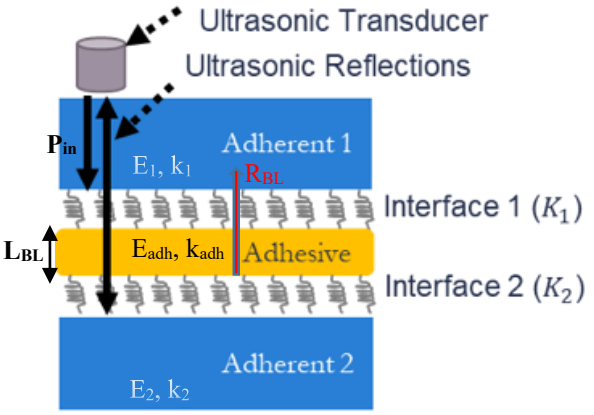


FIGURE 1: PHYSICS-BASED MODEL OF ADHESION

The tri-layer model as given in Equation (1) doesn't take adhesive properties or thickness into account. To take these properties into account, a more thorough analysis of ultrasonic wave reflections from the imperfect interfaces is given in [18] following the modeling framework of Baik and Thompson described in [13]. For a given pair of Young's modulus and wave number E_1, k_1 and E_{adh}, k_{adh} for Adherent 1 and Adhesive respectively, and assuming boundary condition of stress continuity along the interfaces (K_1=K_2=K), the complex phase-dependent reflection coefficient can be written as:

$$R_{BL} = \frac{C_N \cos(k_{adh}L_{BL}) + iS_N \sin(k_{adh}L_{BL})}{C_D \cos(k_{adh}L_{BL}) + iS_D \sin(k_{adh}L_{BL})} \quad (2)$$

$$\begin{cases} C_N = \frac{G_1^2}{K} \\ C_D = 2G_1 G_{adh}\left(1 + \frac{G_1}{K}\right) \\ S_N = G_1^2 - G_{adh}^2 + \left(\frac{G_1 G_{adh}}{K}\right)^2 \\ S_D = G_1^2 + G_{adh}^2 + \frac{G_1 G_{adh}^2}{K}\left(2 + \frac{G_1}{K}\right) \end{cases} \quad (3)$$

where G_1=E_1k_1, G_{adh}=$E_{adh}k_{adh}$ and i=$\sqrt{-1}$.

The unknown adhesive bonding properties can be extracted by fitting the measured phase response of the bondline to the theoretical bondline reflection coefficient modeled in Equations (2) and (3).

[ϕ] Specific vendor and manufacturer names are explicitly mentioned only to accurately describe the test hardware. The use of vendor and manufacturer names does not imply an endorsement by the U.S. Government, nor does it imply that the specified equipment is the best available.

© 2023 by ASME

2.2 Bond Strength Measurement Instrument

NASA's bond strength measurement instrument that is being assessed in this work was built on the CFPLL technology that is described in [15] and succinctly illustrated in Figure 2 [18].

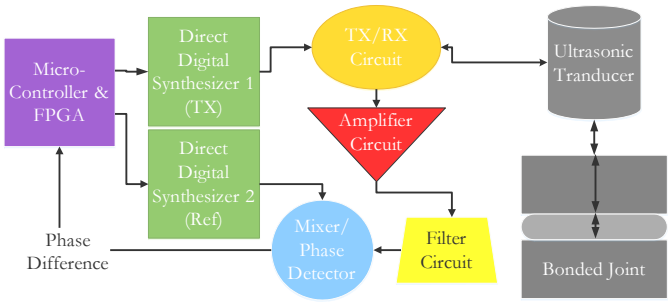


FIGURE 2: PHASE LOCKED LOOP INSTRUMENT

The instrument works on the basic premise of comparing the received ultrasonic waveform reflected from the bonded interface to a reference waveform of the same frequency that has not interacted with the material under test. Comparing the two signals allows measurement of the phase shift in the bonded joint with high resolution and low uncertainty. When this is repeated over a band of frequencies around the anti-resonant frequency of the bondline, the quality of the bond could be inferred from the resulting phase spectral response.

3. SPECIMENS AND DATA COLLECTION

As a proof of concept, to answer the underlying question if this novel phase-based ultrasonic NDE technique can be used to assess bond strength of a bonded joint, simplistic borosilicate (BS) adhesively bonded glass specimens were used in the experiments conducted in [16-19]. The use of these optically transparent specimens, having smooth surfaces and no microstructure, helps to eliminate any confounding effect that may otherwise be present in the experimentations. It also creates a path towards phase-based ultrasonic NDE of metallic bonded joints, where grain noise becomes relevant; and ultimately phase-based ultrasonic NDE of bonded composite joint, where multi-layer laminate and fiber interactions present more complexity. The Gage Repeatability and Reproducibility (Gage R&R) work of the novel phase-based ultrasonic system presented in this paper was performed on these bonded glass specimens produced under various degrading conditions including variations in curing temperature and duration, and contamination of adherent surface, with spray coating of polytetrafluoroethylene (PTFE), prior to bonding.

3.1 Samples for Gage R&R Study

Figure 3 shows a total of 12 samples that were made and deployed in this Gage R&R study. These samples were made of glass adherents cut into coupons measuring on average 5.08 cm x 5.08 cm and 1.10 cm thick. The bondline thicknesses is approximately 100 μm on average.

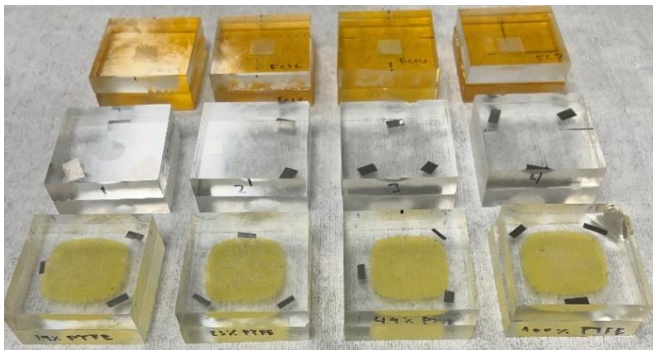


FIGURE 3: TEST SAMPLES FOR THE GAGE R&R STUDY

These samples are representing 3 groups of adherent/adhesive conditions, namely:

1. Epoxy adhesive with varying % of PTFE coverage area
    - PTFE release spray through perforated mask onto the surface of one adherent prior to bonding
2. FM209-1U adhesive with varying thermal conditions
3. UV-cured NOA60 adhesive at varying UV exposure times

Table 1 further describes these samples including the sample ID and conditions of the adhesive as used in this study.

TABLE 1: SAMPLES ID AND ADHESIVE CONDITIONS

ID	Description of Adhesive Condition
Cont19	Epoxy adhesive with 19% PTFE coverage
Cont23	Epoxy adhesive with 23% PTFE coverage
Cont49	Epoxy adhesive with 49% PTFE coverage
Cont100	Epoxy adhesive with 100% PTFE coverage
FC1	FM209-1U fully cured at 250^0F
FC1C	FM209-1U fully cured at 250^0F Contaminated with 20% PTFE coverage
FC1U	FM209-1U under cured adhesive
FC2	FM209-1U fully cured at 350^0F
UV1	NOA60 adhesive with 60 mins UV exposure
UV2	NOA60 adhesive with 180 mins UV exposure
UV3	NOA60 adhesive with 30 mins UV exposure (aged)
UV4	NOA60 adhesive with 60 mins UV exposure (aged)

3.2 Data Collection for Gage R&R Study

Ultrasonic phase measurements were obtained from each of these samples by two separate operators, measuring each sample 3 times in a randomized manner. These measurements were obtained in pulse-echo mode using a highly-damped 10 MHz contact transducer of 0.25" diameter, placed in the center of each sample and held in place using a screw clamp at constant load of ~5 lbs as measured by the load gauge. The transducer was excited with a tone-burst that was swept over a frequency range from 8.5MHz - 11.75MHz in 10kHz step size. The laboratory setup of the ultrasonic phase-based instrument as used in this work is shown in Figure 4.

© 2023 by ASME

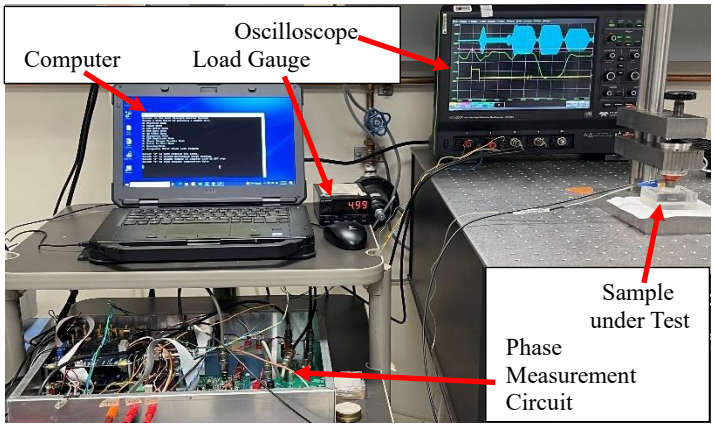


FIGURE 4: ULTRASONIC PHASE-BASED INSTRUMENT

Each operator took out the sample under test from the fixture between measurements and used best practices to reposition the transducer at the center of the sample for a new measurement. Operating in the configuration shown in Figure 4, the computer was used to control the phase measurement circuit, taking phase measurements of the first reflected signal from the adhesive surface at each frequency and recording the measured phase. An example of a reflected waveform is shown in Figure 5 below with the phase information and analysis gate where the phase measurement is obtained.

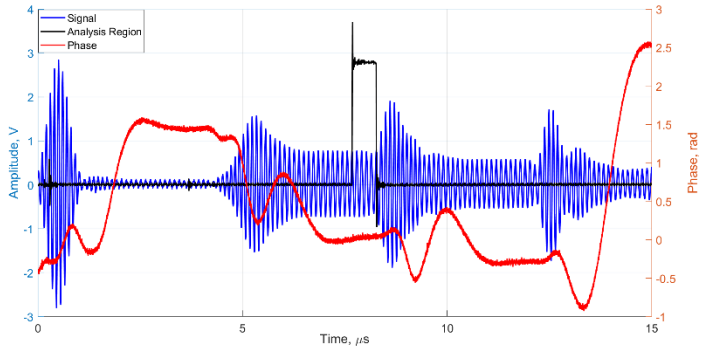
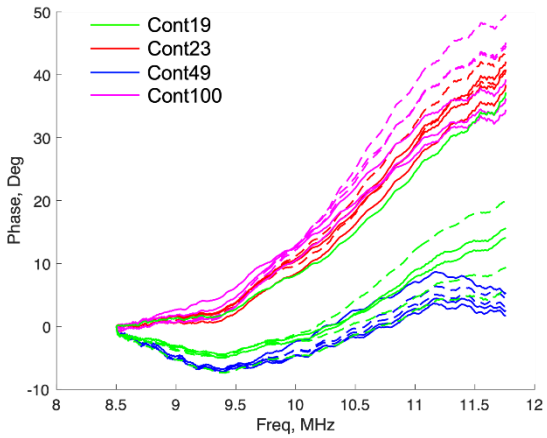
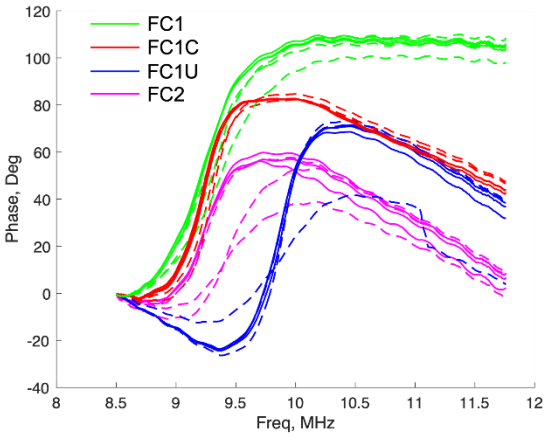


FIGURE 5: EXAMPLE OF A REFLECTED WAVEFORM

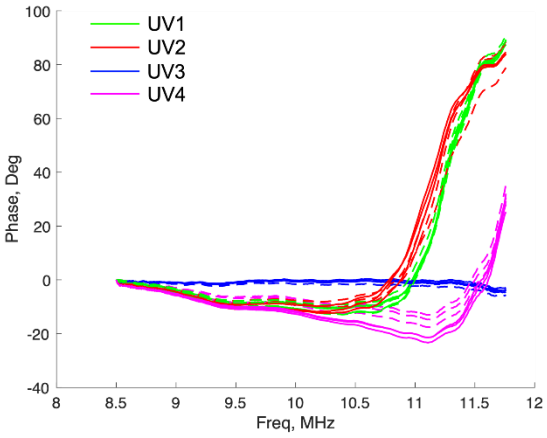
Phase measurements of an unbonded piece of borosilicate were used as a baseline and subtracted from the phase measurements of the bonded sample to respectively determine the relative phase change that is caused by the condition of the bond. Figure 6 shows the phase responses for the three different groups of samples, with samples within each group differentiated by color of the plot. Collected data by each operator for each sample is distinguished by the line patterns (solid vs. dashed lines).



(a) PTFE CONTAMINATED



(b) FM209-1U



(c) NOA60 UV-CURED

FIGURE 6: BONDLINE PHASE REPONSES OF EACH CLASS OF SPECIMENS

As evident from Figure 6, there appear to be some variation in the acquired phase response data, which could be attributed to various sources including but not limited to variations from sample-to-sample, operator-to-operator, temperature, and transducer positioning. Particularly, the variation shown in

© 2023 by ASME

Figure 6a for the PTFE contaminated samples could be readily attributed to the defects in the epoxy adhesive layer as shown in Figure 7.



FIGURE 7: PTFE CONTAMINATED SAMPLE WITH DEFECTS

3.3 Extracted Interfacial Stiffness for Gage R&R Study

Amongst other parameters, the interfacial stiffness *K* was extracted from the measured phase change data by minimizing the difference between this measured phase change and the spring model, described in Section 1 above and in [18], using a nonlinear least-squares approach in Matlab®. An example of a measured phase data curve-fitted with the model described in Equations (2) and (3) is given in Figure 8.

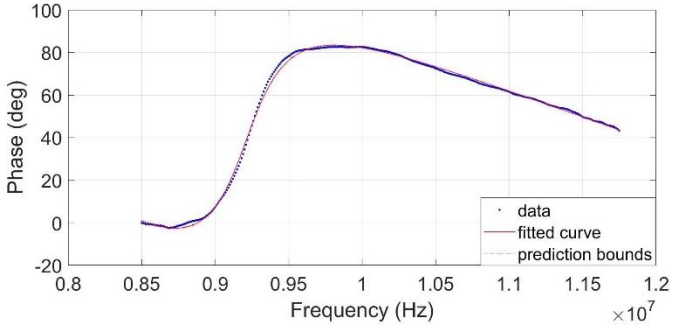


FIGURE 8: EXAMPLE OF FITTED PHASE DATA

A Matlab® routine was written to batch process all 72 measured phase responses (12 samples x 3 replicates x 2 operators) to produce corresponding extracted interfacial stiffness for each measurement. The resulting table of 72 extracted interfacial stiffness data was analyzed using the ANOVA method for the phased-based instrument's measurement repeatability, by the same operator, and reproducibility, by a different operator.

4. GAGE R&R RESULTS AND DISCUSSION

Extracted values of interfacial stiffness *K*, an analog for bond quality, is given by sample and by operator in Figures 9 and 10 respectively.

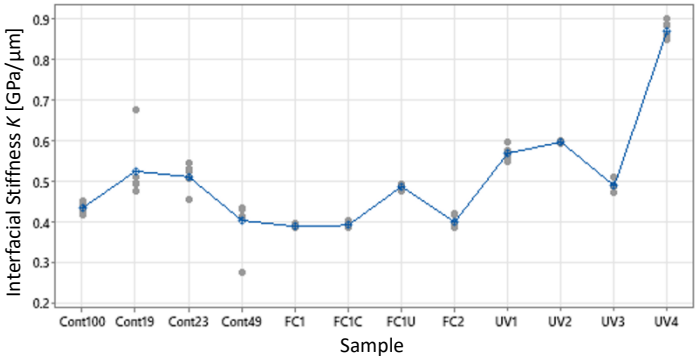


FIGURE 9: EXTRACTED VALUES OF *K* BY SAMPLE

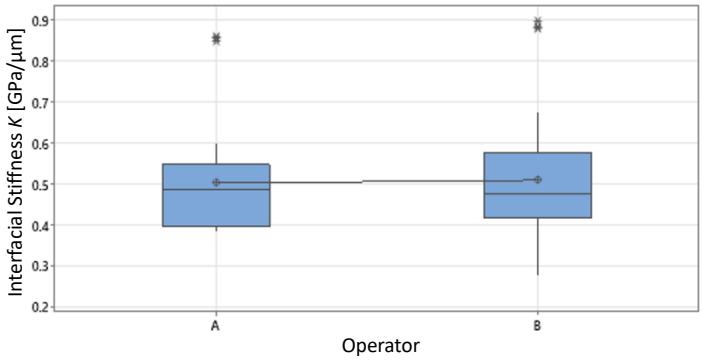


FIGURE 10: EXTRACTED VALUES OF *K* BY OPERATOR

As seen in Figure 9, the measurements of each the PTFE contaminated samples vary noticeably but the other 2 groups of parts were relatively consistently measured. Also, measured averages of all parts vary noticeably, which is desirable as samples used in the study should represent a wide range of values. In Figure 10, we observe that measurement spread for each operator is approximately the same, indicating both operators are measuring the parts similarly. This is again evident in the horizontal line connecting the means of each operator. Also seen in Figure 10 are outliers as measured by each operator.

The measurement inconsistency of the PTFE contaminated samples is again observed in the Sample-Operator Interaction plot illustrated in Figure 11. However, the lines follow very closely for FM209-1U and NOA60 UV-cured samples. The average value of *K* reported is for all replicates of each sample by each operator.

© 2023 by ASME

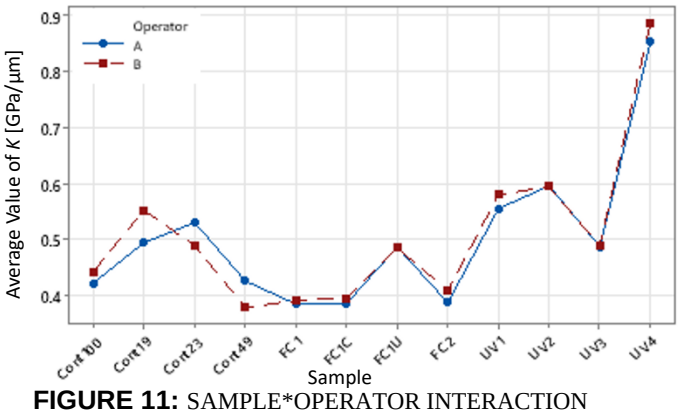


FIGURE 11: SAMPLE*OPERATOR INTERACTION

The reported *p*-value for the sample-operator interaction is 0.212, and using an $\alpha=0.05$ to remove this interaction term from the full model, Minitab® generates Tables 2 and 3 and Figure 12 to show the contribution of each source of variation, respectively as Variance Components (VarComp) and Study Variation (SV).

TABLE 2: VARIANCE COMPONENTS

Source	VarComp	%Contribution (of VarComp)
Total Gage R&R	0.0010034	5.27
Repeatability	0.0010034	5.27
Reproducibility	0.0000000	0.00
Operator	0.0000000	0.00
Part-To-Part	0.0180304	94.73
Total Variation	**0.0190338**	**100.00**

TABLE 3: STUDY VARIATION

Source	Study Var (6 x SD)	%Study Var (%SV)
Total Gage R&R	0.190063	22.96
Repeatability	0.190063	22.96
Reproducibility	0.000000	0.00
Operator	0.000000	0.00
Part-To-Part	0.805663	97.33
Total Variation	**0.827778**	**100.00**

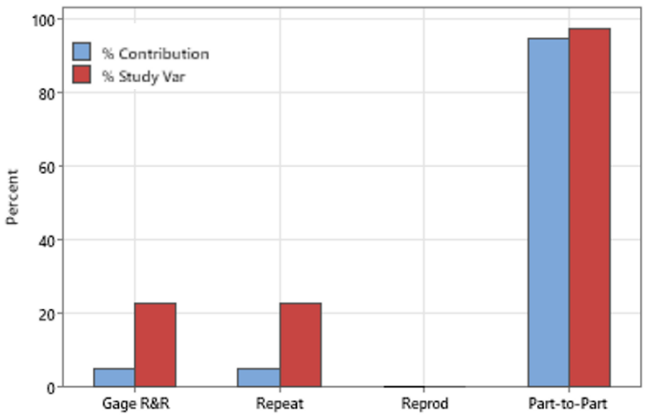


FIGURE 12: COMPONENTS OF VARIATION

Study Variation (SV) reported in Table 3 is obtained from *VarComp* in Table 2 through the Standard Deviation (SD) as:

$$SV = 6 \times \text{SD} = 6 \times \sqrt{VarComp} \quad (4)$$

As given in Table 2, 94.73% of the total variation comes from the Sample-to-Sample variability while the remaining 5.27% is the contribution from the measurement instrument (Total Gage R&R). The Total Gage R&R is from the repeatability error, the error when the same operator is measuring the same sample multiple times with the same instrument. On the other hand, to the number of decimal places rounded here, there is 0% reproducibility error, meaning a different operator can precisely and similarly measure the same samples with the same instrument. According to guidelines published in a manual on Measurement System Analysis by the Automobile Industry Action Group (AIAG) [20], a Total Gage R&R of 10% or lower indicates an acceptable gage.

The reported Number of Distinct Categories is 5, indicating the ability of this novel phase-based bond strength measurement instrument to classify all the measured samples into 5 distinct groups having non-overlapping confidence intervals covering the entire range of the variation of the samples. This parameter is a measure of the variability in the measured samples relative to variability in the measurement instrument. As per AIAG, a gage is considered acceptable when the Number of Distinct Categories is 5 and above [20].

5. CONCLUSION

MSA has been conducted to assess the quality of the novel ultrasonic phase-based bond strength instrument. Specifically, the instrument's precision (repeatability and reproducibility) has been evaluated through a Gage R&R study using the ANOVA method. The study results show this new device can precisely measure interfacial stiffness of adhesively bonded BS specimens with most of the measurement variation coming from the samples instead of the instrument. There's also a chance some of the measurement variations could be due to bondline thickness variation across the samples. While the goal of the instrument is to measure bond strength of composite bonded samples, this study on comparatively simplistic BS specimens provides a roadmap for further development of the laboratory-based instrument to field instrument. With the reproducibility error virtually 0%, for the level of precision reported, the results show the use of such devices could be independent of the operator, making it useful as an in-service equipment to measure bond quality for aerospace parts in use.

However, to get a full picture of the measurement variation of this novel device, an accuracy (bias, linearity, and stability) study is needed. That is a subject for future work.

© 2023 by ASME

ACKNOWLEDGEMENTS

The authors would like to thank the NASA Transformation Tools and Technologies (TTT) project in the Aeronautics Research Mission Directorate for supporting this work.

Minitab® (version 21.2), license owned and hosted by NASA, was used for planning, and analyzing results for the Gage R&R study presented in this paper.

REFERENCES

[1] Parveez, B.; Kittur, M. I.; Badruddin, I. A.; Kamangar, S.; Hussein, M.; Umarfarooq, M.A. *Scientific Advancements in Composite Materials for Aircraft Applications: A Review*. Polymers **2022**, 14, 5007

[2] Ahn, J.; Stapleton S.; Waas A. M. *Advanced Modeling of the Behavior of Bonded Composite Joints in Aerospace Applications.* Composite Joints and Connections, **2011**, 423-434

[3] Omairey, S.; Jayasree, N.; Kazilas, M. *Defects and Uncertainties of Adhesively Bonded Composite Joints: A Review Paper*. Springer Nature Applied Sciences, **2021**, 3, 769

[4] Kumar, R. L. V.; Bhat, M. R.; Murthy, C. R. L. *Evaluation of Kissing Bond in Composite Adhesive Lap Joints using Digital Image Correlation: Preliminary Studies*. Int. J. of Adhesion and Adhesives, **2013**, 42, 60-68

[5] Yan, D.; Neild, S. A.; Drinkwater, B. W. *Modelling and Measurement of the Nonlinear Behavior of Kissing Bonds in Adhesive Joints*. NDT & E Int, **2012**, 47, 18–25

[6] Tattersall, H. G. *The Ultrasonic Pulse-Echo Technique as Applied to Adhesion Testing.* Journal of Physics D: Applied Physics, **1973,** 6, 819-832

[7] Alers, G. A.; Elsley, R. K. *Bond Strength Measurements by Ultrasonic Spectroscopy.* Review of Progress in Quantitative Nondestructive Evaluation, **1978**,

[8] Nagy, P. B. *Ultrasonic Detection of Kissing Bonds at Adhesive Interfaces.* Journal of Adhesion Science and Technology, **1991**, 5(8), 619-630

[9] Lavrentyev, I.; Rokhlin, S. I. *Determination of Elastic Moduli, Density, Attenuation, and Thickness of a Layer Using Ultrasonic Spectroscopy of Two Angles.* Journal of the Acoustical Society of America, **1997**, 102(6), 3467-3477

[10] Rokhlin, S. I.; Wang, L.; Xie, B. *Modulated Angle Beam Ultrasonic Spectroscopy for Evaluation of Imperfect Interfaces and Adhesive Bonds.* Review of Progress in Quantitative Nondestructive Evaluation, **1999**, 18, 1553

[11] Wang. C. H.; Duong, C. N.; *Non-Destructive Evaluation of Bond Quality*, Bonded Joints and Repairs to Composite Airframe Structures, **2016**, 10, 265-285

[12] Cantrell, J., *Hydrogen bonds, interfacial stiffness moduli, and the interlaminar shear strength of carbon fiber-epoxy*. AIP Adv., 2015.

[13] Baik, J.; Thompson, R.; *Ultrasonic Scattering from Imperfect Interface: A Quasi-Static Model*. J. Nondestr. Eval., **1984**

[14] Cantrell, J. *Determination of Absolute Bond Strength from Hydroxyl Groups at Oxidized Aluminum-epoxy Interfaces by ABUS.* J. Appl. Phys., **2004**, 96, 7, 3775-3781

[15] Yost, W. T.; Cantrell, J. H.; Kushnick, P. W. *Fundamental Aspects of Pulse Phase-Locked Loop Technology-based Methods for Measurement of Ultrasonic Velocity.* Journal of the Acoustical Society of America **1992**, 91(3), 1456-1468

[16] Haldren, A. H.; Perey, D. F.; Yost, W. T.; Cramer, K. E.; Gupta, M. C. *Nondestructive Evaluation of Adhesive Bonds via Ultrasonic Phase Measurements.* Proceedings of the 31st Annual Technical Conference of the American Society for Composites, **2016,** 1716-1730

[17] Haldren, H. A.; Perey, D. F.; Yost, W. T.; Cramer, K. E.; Gupta, M. C. *Swept Frequency Ultrasonic Phase Evaluation of Adhesive Bonding in Tri-Layer Structures.* J. Acous. Soc. Amer., **2019**, 145(3), 1609

[18] Haldren, H. A. *Nondestructive Evaluation of Adhesive Bonds by a Novel Ultrasonic Phase Measurement Method*, A Ph.D Dissertation presented to the Faculty at the School of Engineering and Applied Science, University of Virginia, **May 2020**

[19] Webster, M.; Takunju, P. *Phase-Based Ultrasonic Inspection of Aerospace-Grade Adhesive*, Proceedings of the 31st Research Symposium of the American Society of Nondestructive Testing, **2023**, 6, (Under Review)

[20] Automotive Industry Action Group (AIAG). *Measurement Systems Analysis Reference Manual, 4th edition.* **2010**, Chrysler, Ford, General Motors Supplier Quality Requirements Task Force.

© 2023 by ASME